Schecter, Phys. Rev. **138**, B763 (1965); and P. H. Stelson and F. K. McGowan, Phys. Rev. **105**, 1346 (1957).

[4]R. H. Willens, Rev. Sci. Instrum. **33**, 1069 (1962).

[5]F. D. Feiock and W. R. Johnson, Phys. Rev. **187**, 39 (1969).

[6]References 11, 16, and 17 in Paper I.

[7]W. T. Roberts, J. Less-Common Met. **4**, 345 (1962).

[8]R. J. Wasilewski, Trans. Am. Inst. Min. Eng. **221**, 1231 (1961).

[9]J. I. Medoff and I. Cadoff, J. Met. **11**, 581 (1959).

[10]J. Spreadborough and J. W. Christian, Proc. Phys. Soc. Lond.

74, 609 (1959).

[11]R. L. P. Berry and G. V. Raynor, Research **6**, 215 (1953).

[12]R. H. Willens (private communication). The data of Willens have, in addition, given best agreement with the interpretation of data on the pressure derivatives of the elastic moduli of Ti according to E. S. Fisher and M. H. Manghnani, J. Phys. Chem. Solids **32**, 657 (1971).

[13]P. Raghavan, R. S. Raghavan, E. N. Kaufmann, K. Krien, and R. A. Naumann, Bull. Am. Phys. Soc. **18**, 134 (1973).

Electric Field Gradient at Ta in Group-IVB Metals. III. ω-Zirconium

E. N. Kaufmann and D. B. McWhan

Bell Laboratories, Murray Hill, New Jersey 07974

(Received 26 February 1973)

Using the time-differential perturbed-angular-correlation technique, we have observed the nuclear-electric-quadrupole interaction at ^{181}Ta(482 keV) as an impurity in the ω-phase modification of Zr metal. The measured interaction frequencies for the two crystallographically inequivalent sites are $\nu_Q^A = 280 \pm 2$ MHz and $\nu_Q^B = 382 \pm 2$ MHz, which correspond to electric field gradients of $|eq^A| = (4.58 \pm 0.19) \times 10^{17}$ V/cm^2 and $|eq^B| = (6.24 \pm 0.25) \times 10^{17}$ V/cm^2, respectively. We find that the ratio of field gradients is in remarkably good agreement with results of a point-ion lattice-sum calculation and the gradient magnitudes support a reduced-valence picture of the ω structure.

INTRODUCTION

Measurements of the principal component of the electric field gradient eq at Ta in α-phase zirconium[1] and titanium[2] metals have been reported in two companion papers (henceforth denoted I and II, respectively). The α phase of these group-IVB transition metals displays the hexagonal-close-packed (hcp) crystal structure at normal temperatures and pressures. Under high hydrostatic pressure, however, a transformation to the so-called ω-phase structure occurs in both metals.[3] As an extension of the previously reported work, we have undertaken the measurement of eq at Ta in ω-zirconium.

The ω phase offers a variation in the approach to the study of field gradients in metals which was not available in the hcp structures. Two crystallographically inequivalent atomic sites, occupied in the ratio 2:1, are present in the ω structure. It is therefore possible to determine two separate field-gradient values in a single elemental environment and to specifically associate each value with its corresponding lattice site by exploiting the known 2:1 occupancy ratio. The relative size of eq at the two sites may be a more useful quantity for comparison with lattice-sum calculations than the absolute magnitude at a single site.

Crystal Structure of ω Phase

The ω-phase lattice shows the C32-type hexagonal structure (typified by the compound AlB$_2$) with space group P6/mmm.[3,4] This structure contains three atoms per unit cell. Referring to hexagonal axes (internal angle 120° in the basal plane), one atom site (A) at the origin $(0, 0, 0)$ has coordination number 14 and two equivalent sites (B) at $(\frac{1}{3}, \frac{2}{3}, \frac{1}{2})$ have coordination number 11. The ideal axial ratio (c/a) of the lattice is $c/a = \sqrt{\frac{3}{8}} \approx 0.612$ for packing of hard spheres. Figure 1(a) gives a view of the relative atomic positions in the unit cell. Figures 1(b) and 1(c) present projections of the lattice positions on the basal plane with site A and site B regarded as the origin, respectively.

Previously measured lattice-constant values for ω-zirconium[3] are $c = 3.109$ Å and $a = 5.036$ Å, which yield a nearly ideal axial ratio of $c/a = 0.617$. We emphasize here that sites of type A and B display different point symmetries (6/mmm and $\bar{6}m2$, respectively) and markedly different coordination numbers. It might be reasonable to expect on this basis a significant difference in the electronic contribution to the electric field gradient at A and B sites. Further consideration of this possibility will be included with the discussion of the experimental results.
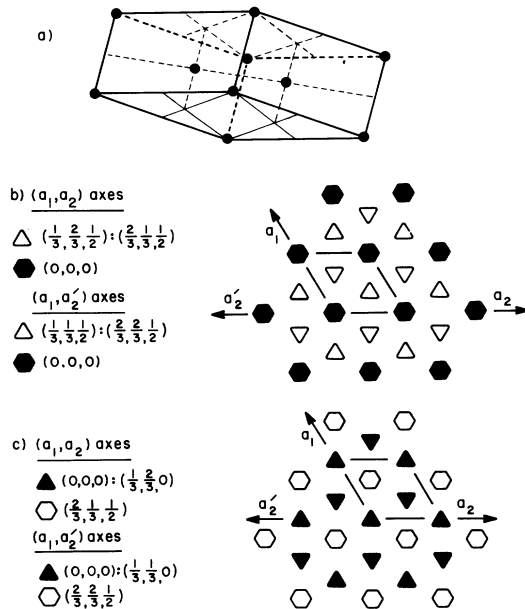
FIG. 1. (a) Unit cell of the ω structure with A-type sites at corners and B-type sites in the midplane. (b) Projection of ω-phase atom positions on the basal plane with an A-type site at the origin of coordinates. Hexagons and triangles refer to the hexagonal and trigonal point symmetry at A- and B-type sites, respectively. Solid symbols represent atoms in the plane of the origin and open symbols represent atoms in the plane $z = c/2$. (c) Same as (b) but with a B-type site at the origin.

EXPERIMENTAL TECHNIQUE

Samples of the same 1-at.% Hf in Zr alloy foil which was used in the study of α-zirconium described in I were employed in the form of disks of $\frac{1}{8}$- and $\frac{1}{4}$-in. diameter and 0.002-in. thickness. These were irradiated with pile neutrons to form the desired [181]Hf radioactivity for the time-differential perturbed-angular-correlation (TDPAC) measurements. A most convenient feature of the transformation of zirconium to the ω phase under pressure is the metastable retention of that phase at atmospheric pressure and room temperature. It was thus feasible to produce the ω structure in a separate procedure and to avoid the unfavorable geometry and radiation scattering and absorption introduced by mating a high-pressure device directly to the angular-correlation apparatus. Each irradiated sample was placed in a pressure cell of the Bridgman opposing-anvil type using an iso-mica annular retention gasket and AgCl as the pressure-transmitting medium. For all samples save one, a pressure in excess of 100 kbar was maintained for several hours to ensure complete transformation and then released slowly. One sample was brought to only 40 kbar (i.e., below the ~ 60-kbar transition pressure) in order to see the effects of pressurization on the α phase.

One of the transformed samples was accompanied in the cell by an inactive sliver of the same foil which was subsequently subjected to x-ray diffraction analysis. The x-ray results verified transformation to the ω phase and determined the lattice parameters to be $c = 3.135 \pm 0.001$ Å, $a = 5.042 \pm 0.001$ Å and $c/a = 0.622$. These values differ somewhat from those of Jamieson,[3] perhaps because of the 1-at.% Hf alloy used or the presence of small amounts of other impurities (see note added in proof).

For measurements at room temperature, samples prepared as described above were mounted on a revolving shaft at the center of the angular-correlation apparatus. The rotation of the sample served to present an effectively cylindrically symmetric source to the radiation detectors. A variable-temperature liquid-He-flow cryostat and a glass helium Dewar were used at various times for measurements below room temperature. In all respects, the detectors, electronics and data acquisition systems, and techniques were identical to those previously described in Paper I.

The data analysis proceeded along similar lines to that described in I; however, account had to be taken of two distinct field gradients and therefore two quadrupole precession frequencies corresponding to sites A and B of the ω phase. To accomplish this, the function given by Eq. (4) of Paper I was assumed to apply to each site separately. Two such functions were added in the ratio 2:1 to form a function which would be fitted to the data. Only the nuclear lifetime τ_N, the experimental time zero t_0, and a total zero-frequency amplitude c_0 were common to both sites. The relative amplitudes of the harmonic-frequency terms, the axial asymmetry parameters, and the frequency distribution widths were allowed to vary independently for each site A and B.

RESULTS

A typical TDPAC spectrum is shown in Fig. 2 where it is immediately obvious that two frequencies are present and that the higher frequency makes the stronger contribution to the spectrum. Thus we can associate the higher frequency with site B and the lower with site A. The solid curve in the figure is the result of least-squares fit to the function presented in Paper I modified as described in the preceding section. The nuclear decay factor has been removed from both the data and the fitted curve. The quadrupole frequencies $\nu_Q = e^2 Qq/h$, extracted from a weighted average of results for three separate runs at room temperature are $\nu_Q^A[$[181]Ta(482 keV) in ω Zr$] = 280 \pm 2$ MHz and $\nu_Q^B = 382 \pm 2$ MHz. Frequencies for sample temperatures other than room temperature are included
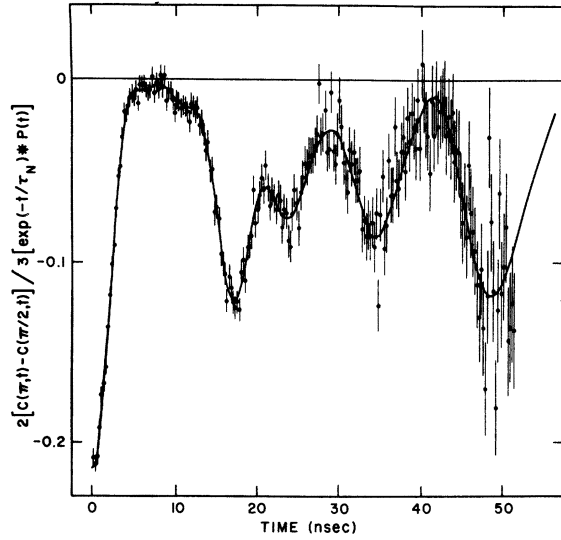
FIG. 2. Typical experimental time spectrum for the TDPAC anisotropy with the nuclear decay factor removed. The solid curve is the result of a least-squares fit as described in the text.

in Fig. 3 and the tabulation of results in Table I. In all instances for both sites A and B the fitted values of the asymmetry parameter $\eta = (V_{xx} - V_{yy})/V_{zz}$ satisfied $\eta \leq 0.15$ and the relative frequency dis-
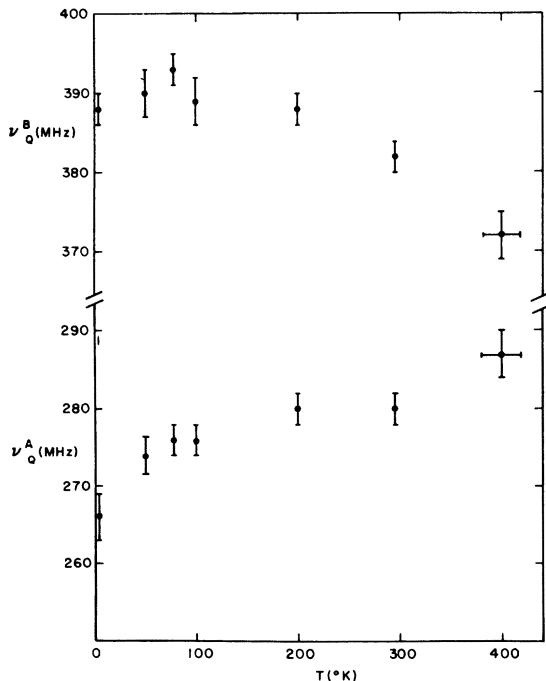
TABLE I. Results for the quadrupole frequency $\nu_Q = e^2qQ/h$ at various temperatures.

$T(^\circ K)$	ν_Q^A(MHz)	ν_Q^B(MHz)
4	266(3)	388(2)
50	274(2)	390(3)
77	276(2)	393(2)
100	276(2)	389(3)
200	280(2)	388(2)
296	280(2)	382(2)
400(20)[a]	287(3)	372(3)

[a] A failure in a thermocouple limited the accuracy of the temperature measurement to $\pm 20\,^\circ$K at $400\,^\circ$K.

tribution width was $2\sigma/\omega \leq 0.03$.

The data obtained for the sample which was raised only to 40-kbar pressure were fitted well by a single frequency consistent with that found for the α phase in Paper I, indicating that a transition to the ω phase had not occurred. The only discernible effect of the applied pressure on this sample was an increase in the width of the frequency distribution by about a factor of 2.

By inserting the value of the nuclear quadrupole moment of the 482-keV state of ^{181}Ta ($Q = 2.53 \pm 0.10$ b)[5] into the expression for ν_Q, we find the values of the field gradients at Ta in ω Zr at room temperature to be

$$|eq^A| = (4.58 \pm 0.19) \times 10^{17} \text{ V/cm}^2$$

and   (1)

$$|eq^B| = (6.24 \pm 0.25) \times 10^{17} \text{ V/cm}^2 \; .$$

The ratio of quadrupole frequencies, which is unaffected by the uncertainty in the nuclear quadrupole moment, gives $|q^B/q^A| = 1.36 \pm 0.01$. As is evident from Fig. 3, ν_Q^A and ν_Q^B approach each other as the temperature is raised and the gradient ratio is therefore a weakly decreasing function of temperature.

DISCUSSION

Before trying to extract from the above results information regarding the relative contributions to $|eq|$ of ions on lattice points and of electrons in the metal, a calculation of the lattice contribution is necessary. To our knowledge, no lattice-sum calculations are available for the ω-phase structure, although such calculations have been done for hcp lattices by de Wette[6] and general formulas useful for lattices of arbitrary symmetry have been presented by de Wette and Schacher.[7] We have undertaken the computation of the appropriate lattice sums for the ω structure following the techniques described in Refs. 6 and 7. The details of the computation are given in the Appendix. For the axial ratio $c/a = 0.622$ measured on our test
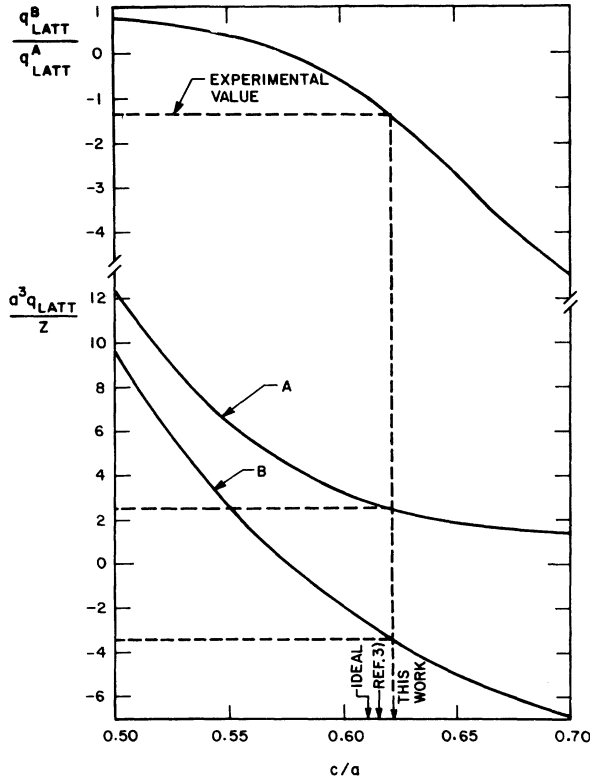

FIG. 3. Experimentally determined values of the quadrupole frequencies for sites A and B at various sample temperatures. Corresponding numerical values may be found in Table I.

FIG. 4. Values of the reduced field gradients for sites A and B and their ratio vs the axial ratio c/a as calculated in the Appendix for a point-ion lattice under the assumption of equal ionic charges $(Z_A = Z_B)$. The dashed lines show the precise correspondence of the measured gradient ratio to the measured axial ratio.

sample, the lattice-sum evaluation yields the reduced (dimensionless) gradients

$$a^3 q^A_{1att}/Z = +2.484$$

and   (2)

$$a^3 q^B_{1att}/Z = -3.431 ,$$

where a is the lattice constant in the basal plane and Z is the ionic charge assumed to be centered at all lattice sites. The magnitude of the ratio $q^B_{1att}/q^A_{1att} = -1.38$ is in remarkably good agreement with the experimental value.

To show that this agreement does not simply arise from an insensitivity of the ratio to the adopted value of c/a or to the assumption of equal ionic charges at all lattice sites, the lattice sums were evaluated for a wide range of axial ratios and also for various values of the ratio of ionic charge on B sites (Z_B) to that on A sites (Z_A). Figure 4 shows the dependence of the reduced lattice gradients and their ratio on c/a under the assumption that $Z_A = Z_B$. The figure demonstrates that the lattice gradient ratio is a sensitive function of c/a and that it is therefore unlikely that the precise

correspondence of the measured gradient ratio to the experimentally determined value of c/a is accidental. Whereas only the magnitude of the gradient ratio has been determined experimentally, a negative sign is strongly suggested by the agreement with the lattice-sum prediction.

To explore the effect of relaxing the assumption that $Z_A = Z_B$, we plot in Fig. 5(a) the lattice-sum results as a function of the site-B to site-A ionic charge ratio (Z_B/Z_B) for a few values of c/a around 0.622. As shown in this figure, the lattice gradient ratio is extremely sensitive to Z_B/Z_A in the region of interest because of the vanishing of q^A_{1att} near $Z_B/Z_A \approx 1.25$. The precise correspondence of the measured gradient ratio to the charge ratio $Z_B/Z_A = 1.00$ then lends additional support to the notion that agreement with the lattice-sum calculation is not accidental.

It is however also evident that relaxing the assumption of equal ionic charges on sites A and B allows the possibility of agreement with a positive gradient ratio for a charge ratio of $Z_B/Z_A = 1.46$. The curves displayed in Fig. 5(b) show the relation between Z_B/Z_A and c/a required by a given value of q^B_{1att}/q^A_{1att}. These demonstrate that, even for the unreasonably large uncertainty in c/a of 1%, knowledge of the lattice gradient ratio restricts Z_B/Z_A to two well-defined regions about 1.0 and 1.5 for negative and positive ratio values, respectively. Thus, in addition to the reduced lattice gradient values of Eq. (2) for the case $q^B_{1att}/q^A_{1att} < 0$ and $Z_A = Z_B$, we should consider the following set for the possibility $q^B_{1att}/q^A_{1att} > 0$ and $Z_B/Z_A = 1.46$:

$$a^3 q^A_{1att}/Z_A = -2.016$$

and   (3)

$$a^3 q^B_{1att}/Z_A = -2.779 ,$$

where we have chosen to normalize to the charge at site A. It is of course quite clear from Fig. 5(a) that once the restriction $Z_B = Z_A$ is relaxed, virtually any experimentally determined gradient ratio could be reproduced by the lattice-sum result if an appropriate value of Z_B/Z_A is assumed. It is therefore necessary to invoke some knowledge of the physical properties of the system to decide which solution is most reasonable or in fact whether it is even reasonable to expect a lattice-sum calculation, which ignores local electronic effects, to agree with experiment.

Past experience with field gradients at nuclei in metallic environments has indicated that electronic effects may cause large discrepancies between measured and lattice-sum results even after taking account of atomic antishielding factors.[8] On the other hand, since the field gradient does, in the last analysis, arise from deviations of the lat-

a)

c/a = 0.635 — —
0.622 ———
0.612 - - - - -

$\dfrac{Z_B}{Z_A}$

2.0

1.5

1.0

0.5

0

-3 -2 -1 0 +1 +2

q^B_{LATT}/q^A_{LATT}

b)

+1.28
+1.38
+1.48

q^B_{LATT}
q^A_{LATT}

-1.48
-1.38
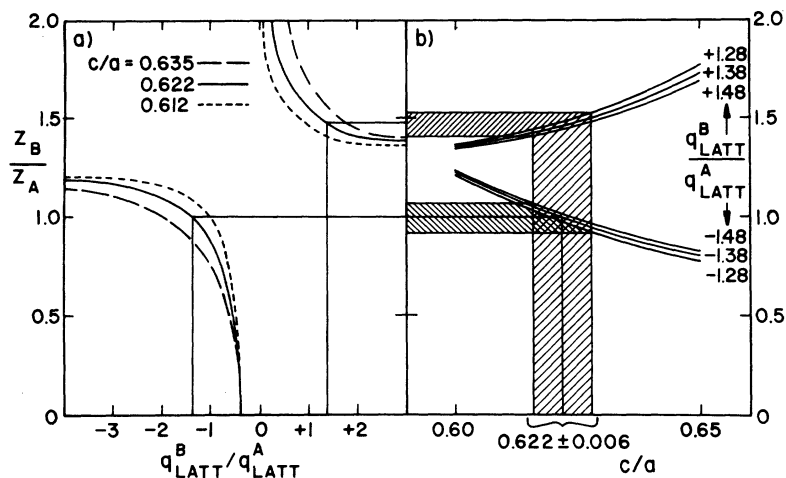-1.28

2.0

1.5

1.0

0.5

0

0.60 0.622±0.006 0.65

c/a

FIG. 5. (a) The ionic charge ratio needed to yield a given lattice gradient ratio from the point-ion calculation given in the Appendix. A few choices of the axial ratio parameter near the measured value are shown. (b) Using the calculated lattice gradient ratio as a parameter, the dependence of assumed ionic charge ratio on the axial ratio is shown. The shaded regions show the uncertainty introduced in Z_A/Z_B by arbitrarily assuming a 1% error in the measured axial ratio.

tice structure from cubic symmetry, it may be physically plausible to assume under some circumstances that all contributions to that gradient are at least proportional to the lattice gradient. The agreement of the calculated and measured gradient ratio for the case $Z_A = Z_B$ would indicate that this is the case for ω-Zr and that the proportionality factors applicable to sites A and B are identical. The choice $Z_A = Z_B$ is also supported by considering the fact that ω-Zr is a metal with mobile conduction electrons which would redistribute themselves in such a way as to counterbalance any tendency of planes of A-type and B-type ions to maintain different ionic charges. In fact, since the point-ion lattice-sum calculation given in the Appendix assumes a *uniform* background of electronic charge in order to maintain over-all charge neutrality, a spatial redistribution of the electrons lies outside the scope of that calculation and relaxing the $Z_A = Z_B$ condition is therefore a mathematical rather than physical artifice. The acceptance of this argument and of the *negative* gradient ratio solution, however, still rests on our belief that the agreement of the gradient ratio with the lattice calculation, using the measured c/a value and the unique condition $Z_A = Z_B$, is not due to a fortuitous combination of local electronic effects unrelated to eq_{latt}.

Prior to the completion of the calculations it had been expected, based on the recent work of Doherty and Gibbons,[9] that lattice-sum results would not agree well with experiment. In Ref. 9 it was concluded that in ω-Zr, fewer electrons are contributed to the conduction band by B-type sites than by A-type sites and that the electrons retained at a B-type site were involved in highly directional covalent bonding with the three near-neighbor atoms in the same plane. They proposed that the electronic wave function describing these trigonal bonds

would be derived from the hybridization of s and d orbitals. We had expected, therefore, that if the Ta impurity, at which we measure the field gradients, participated in this bonding scheme through its $5d$ electrons, then a large contribution to the field gradient at a B-type site over that expected from the lattice would be observed. This was not borne out by our results.

The suggestion that fewer than four electrons per atom are donated to the conduction band was supported by unpublished magnetic susceptibility measurements.[9] Jamieson,[3] in fact, had pointed out that if the distance of closest approach in the ω structure is inserted in a relation given by Pauling[10] between coordination number, atomic radius, and "valence," then a valence of $Z = 3$ is strongly indicated for ω-Zr. The formation of the ω phase in Zr-Nb alloys which would otherwise have too great an electron-to-atom ratio is consistent with this reduced-valence picture. By considering the magnitudes of our measured field gradients, we can hope to decide between $Z = 4$ and $Z = 3$.

In order to compare the results of Eq. (1) with the lattice-sum calculation, we must assume a value for the Sternheimer antishielding factor[8] applicable to the Ta ion. Lacking precise knowledge of the Ta charge state and the effect of the metallic environment, we have used the value for $(1 - \gamma_\infty)$ of 62 for the Ta^{5+} ion given by Feiock and Johnson.[11] Even for the free ion, this value may be 5–10% in error and, as shown by Pelzl[12] for the rare earths, may be significantly affected by metallic surroundings. Nevertheless, the comparison of entries in Table II, where the lattice-sum prediction of Eq. (2) for $Z = 3$ and 4 are given along with the values of Eq. (1), favors the valence $Z = 3$ in agreement with expectations.[3,9] One might argue, based on this evidence, that a Ta^{4+} charge state should have been assumed initially. This would

TABLE II. Comparison of the experimental field gradient values with lattice-sum predictions for $Z = 3$ and 4. All quantities are given in units of 10^{17} V/cm^2.

		Site A	Site B
$\lvert eq_{\text{expt}} \rvert$		4.58 ± 0.19	6.24 ± 0.25
$(1 - \gamma_\infty) eq_{\text{latt}\,a}$	$Z = 3$	$+5.21$	-7.18
	$Z = 4$	$+6.94$	-9.57

[a]Lattice-sum results computed assuming $Z_A = Z_B$ and a Sternheimer antishielding factor of $(1 - \gamma_\infty) = 62$.

imply an unpaired electron in the $5d_{3/2}$ orbital of the Ta ion. Although it has been shown[11] that $d_{3/2}$ subshells contribute to $(1 - \gamma_\infty)$ in such a way as to reduce its value slightly, the electric field gradient from a single $5d$ electron, which is of the order of 3×10^{18} V/cm^2, would overshadow this effect. Our measurements provide no evidence to support this possibility.

Near perfect agreement with the measurement could be obtained if the factor $(1 - \gamma_\infty)$ were reduced by only ~10% for the $Z = 3$ results of Table II. Alternatively, the value of Z, the ionic charge per atom, may be reduced to ~2.65, since there is no requirement that Z be integral. This value of Z would imply a total effective ionic charge per unit cell of $Z_A + 2Z_B = 8$. The uncertainties in the values of $(1 - \gamma_\infty)$ and Z, however, leave their individual determination in doubt and only the total enhancement factor $q_{\text{expt}}/(q_{\text{latt}}/Z) = 163 \pm 5$ can be quoted with confidence.

To our knowledge no measurements of the lattice constants of ω-Zr as a function of temperature are available. The rather weak dependence of the field gradients (cf. Fig. 3) on temperature, however, supports the idea that contributions to eq from electrons near the Fermi level are not significant. The decrease of the gradient ratio with temperature when compared with Fig. 4 would indicate that c/a increases with temperature.

SUMMARY

We have measured the electric field gradients acting on Ta impurity nuclei at both sites in ω-Zr and have found that the ratio of the gradients is in excellent agreement with the prediction of lattice-sum calculations in which equal ionic charges are assumed to reside at all Zr lattice sites. We have rejected alternative lattice-sum results which, in order to match experiment, require unequal charges at the two inequivalent sites because charge separation seemed physically unacceptable for a metallic environment and because it seemed highly likely that the excellent agreement with the equal-charge assumption was not accidental. The results imply that all electronic contributions to

the field gradient are proportional to the lattice gradient with identical proportionality factors at each site. Our measurements also support the reduced-valence scheme for the ω phase proposed by Jamieson[3] and Doherty and Gibbons.[9] The lack of any dramatic dependence of the results on temperature supports the notion that conduction electrons near the Fermi surface do not contribute strongly to the field gradient. A critical test of the validity of our assumptions must await additional measurements such as nuclear-quadrupole-resonance studies on ^{91}Zr in ω-Zr or Mössbauer-effect measurements on ^{181}Ta in ω-Zr, the latter of which would be sensitive to the sign of the quadrupole interaction.

Note added in proof. A recent private communication from J. C. Jamieson has indicated a revised value of the axial ratio $c/a = 0.622$, in agreement with the result quoted here.

APPENDIX

We follow below the planewise summation method described by de Wette[6] and de Wette and Schacher[7] and references therein. The notation used will be identical to theirs and will not be exhaustively described below. In order to duplicate the notation for hexagonal lattices of Refs. 6 and 7 exactly, we will use hexagonal axes a_1 and a_2' in the basal plane with interior angle 60°. In this system (cf. Fig. 1), the ω structure has lattice points at $(0, 0, 0)_A$, $(\frac{1}{3}, \frac{1}{3}, \frac{1}{2})_B$, and $(\frac{2}{3}, \frac{2}{3}, \frac{1}{2})_B$ when referred to an A-type site as origin of the unit cell. The subscripts on the basis vectors denote the type of site (A or B). Since the lattice sums to be evaluated will give the contributions from each of the three hexagonal sublattices to the field gradient at the origin, to find the gradient at a B-type site we must also use the basis coordinates with respect to a B-site origin, i.e., $(0, 0, 0)_B$, $(\frac{1}{3}, \frac{1}{3}, 0)_B$, and $(\frac{2}{3}, \frac{2}{3}, \frac{1}{2})_A$.

The expression appropriate to a metallic lattice, with a uniform background of electronic charge to ensure over-all charge neutrality, is

$$eq = (8\pi e/3V) \sum_j Z_j + e \sum_j Z_j S_{j_1 j_2 j_3} \qquad (A1)$$

for the zz component of the electric field gradient at the origin with respect to which the basis indices j_i are referred. We have generalized de Wette's formula to the extent that different charges Z_j are allowed for each sublattice j even though a metal is under consideration. The unit cell volume is $V = \frac{1}{2}\sqrt{3}\, a^3 \alpha$ where we define α as the axial ratio c/a. Writing out the explicit expressions for the two ω-phase sites results in

$$eq^A = \frac{16\pi}{3\sqrt{3}} \frac{(Z_A + 2Z_B)e}{a^3 \alpha} + eZ_A S_{000}$$

$$+ eZ_B S_{\frac{1}{3}\frac{1}{3}\frac{1}{2}} + eZ_B S_{\frac{2}{3}\frac{2}{3}\frac{1}{2}} \quad \text{(A2a)}$$

and

$$eq^B = \frac{16\pi}{3\sqrt{3}} \frac{(Z_A + 2Z_B)e}{a^3 \alpha} + eZ_B S_{000}$$

$$+ eZ_B S_{\frac{1}{3}\frac{1}{3}0} + eZ_A S_{\frac{2}{3}\frac{2}{3}\frac{1}{2}} \quad . \quad \text{(A2b)}$$

Since it is easily demonstrated from the expression for $S_{j_1 j_2 j_3}$ in Ref. 6 that $S_{\frac{2}{3}\frac{2}{3}\frac{1}{2}} \equiv S_{\frac{1}{3}\frac{1}{3}\frac{1}{2}}$, we are left with only three sublattice sums to evaluate, namely, S_{000}, $S_{\frac{1}{3}\frac{1}{3}0}$, and $S_{\frac{1}{3}\frac{1}{3}\frac{1}{2}}$.

Considering the last sum first, de Wette[6] gives the formula for $S_{\frac{1}{3}\frac{1}{3}\frac{1}{2}}$, since it is also applicable to hcp lattices, as the following sum over a planar hexagonal lattice in reciprocal-lattice space:

$$S_{\frac{1}{3}\frac{1}{3}\frac{1}{2}} = \frac{8\pi^2}{\sqrt{3}\, a^3} \sum_{\mu_1 \mu_2} \exp\left[-\tfrac{2}{3}\pi i(\mu_1 + \mu_2)\right]$$

$$\times \frac{h_{\mu_1 \mu_2}}{\sinh(\pi h_{\mu_1 \mu_2} \alpha)} \quad . \quad \text{(A3a)}$$

As shown in Ref. 6, this can be rewritten as a sum over shells, defined by lattice points having the same magnitude of reciprocal-lattice vector $|\vec{h}_{\mu_1 \mu_2}|$,

$$S_{\frac{1}{3}\frac{1}{3}\frac{1}{2}} = \frac{8\pi^2}{\sqrt{3}a^3} \sum_i \frac{n_i h_i c_i}{\sinh(\pi h_i \alpha)} \quad . \quad \text{(A3b)}$$

The shell populations n_i, phase factors c_i, and vector lengths h_i have been tabulated by de Wette[6] for the first twelve shells. Where appropriate below we shall write sums only in the form corre-

sponding to Eq. (A3b) rather than Eq. (A3a).

Because the remaining two sums to be evaluated display a third index $j_3 = 0$, a special problem arises. It turns out[7] that the transformation to reciprocal space (two-dimensional Fourier transform), which is the basis of the well-conditioned convergence of the summation technique, will be undefined for that atomic plane of the direct-space sublattice which contains the origin. In Ref. 7 it is shown how the offending term can be evaluated separately by a direct-lattice summation with the aid of an auxiliary convergence function. The sums are written in two parts as

$$S_{j_1 j_2 0} = S_{j_1 j_2 0}^{\lambda_3} + S_{j_1 j_2 0}^0 \quad , \quad \text{(A4)}$$

where the second term requires special attention.

The first term may be written immediately as

$$S_{000}^{\lambda_3} = \frac{8\pi^2}{\sqrt{3}a^3} \sum_i \frac{n_i h_i \exp(-\pi h_i \alpha)}{\sinh(\pi h_i \alpha)} \quad , \quad \text{(A5)}$$

which is also given by de Wette[6] for hcp lattices, and

$$S_{\frac{1}{3}\frac{1}{3}0}^{\lambda_3} = \frac{8\pi^2}{\sqrt{3}a^3} \sum_i \frac{n_i h_i c_i \exp(-\pi h_i \alpha)}{\sinh(\pi h_i \alpha)} \quad , \quad \text{(A6)}$$

which is peculiar to the ω structure and differs from Eq. (A5) only in the phase factors c_i. The reader is referred to Ref. 7 for the details of evaluating the second terms of Eq. (A4). The results are

$$S_{000}^0 = -\frac{1}{a^3}\left(-\frac{4\pi}{3} + \frac{8\pi}{\sqrt{3}} + \frac{2}{\sqrt{\pi}}\sum_{\lambda_1 \lambda_2}' \Gamma(\tfrac{3}{2}, \pi\sigma_\lambda^2)\sigma_\lambda^{-3}\right.$$

$$\left. + \frac{4\pi\sqrt{\pi}}{\sqrt{3}}\sum_i n_i h_i \Gamma(-\tfrac{1}{2}, \pi h_i^2)\right) \quad \text{(A7)}$$

and

TABLE III. Tabulation of selected lattice sums for the ω phase.

c/a	$-a^3 S_{\frac{1}{3}\frac{1}{3}\frac{1}{2}}$	$a^3 S_{\frac{1}{3}\frac{1}{3}0}^{\lambda_3}$	$a^3 S_{000}^{\lambda_3}$	$a^3 q^A/Z$ [a]	$a^3 q^B/Z$ [a]
0.20	16.7813	−47.3761	529.256	696.888	609.580
0.30	−34.8281	−25.2081	140.599	156.644	143.114
0.40	−33.9012	−13.4748	49.8835	43.5989	40.8747
0.50	−27.4957	−7.09920	20.4699	12.4859	9.73187
0.55	−24.4068	−5.10645	13.5287	6.44592	2.59578
0.60	−21.5563	−3.65176	9.06291	3.28407	−1.96191
0.612	−20.9093	−3.36674	8.24517	2.81195	−2.79602
0.617	−20.6440	−3.25438	7.92786	2.64108	−3.11988
0.622	−20.3811	−3.14561	7.62344	2.48431	−3.43075
0.65	−18.9545	−2.59809	6.13169	1.83595	−4.95821
0.70	−16.5949	−1.84037	4.17882	1.41306	−6.98292
0.80	−12.5608	−0.914039	1.96956	2.08973	−9.41403
0.90	−9.35936	−0.449602	0.939441	3.43186	−10.8089
1.00	−6.87941	−0.219794	0.451037	4.67884	−11.8121
1.10	−4.99941	−0.107037	0.217332	5.56687	−12.6913
1.20	−3.59976	−0.052002	0.104932	6.05522	−13.5476
1.5926	−0.935175	−0.003027	0.006061	5.32381	−16.8946

[a]Computed assuming equal charges at all sites.

$$S^0_{\frac{1}{3}\frac{1}{3}0} = -\frac{1}{a^3}\left(\frac{8\pi}{\sqrt{3}} + \frac{2}{\sqrt{\pi}}\sum_{\lambda_1\lambda_2}\Gamma(\tfrac{3}{2},\pi\sigma^2_{\lambda,j})\sigma^{-3}_{\lambda,j}\right.$$

$$\left. + \frac{4\pi\sqrt{\pi}}{\sqrt{3}}\sum_i n_i h_i c_i \Gamma(-\tfrac{1}{2},\pi h_i^2)\right) \ . \quad (A8)$$

The $\Gamma(n, x)$ are the incomplete Γ functions, the sum over $\lambda_1\lambda_2$ is on a direct-space planar hexagonal lattice, and $\sigma_{\lambda,j}$ are magnitudes of vectors from the origin to the points of that lattice. Note that in Eq. (A7) the $\lambda_1 = \lambda_2 = 0$ term is excluded from the sum whereas it is included in Eq. (A8). Both Eq. (A7) and Eq. (A8) are independent of the axial ratio α and are therefore simply numbers whose value need be calculated only once. Since Eq. (A7) also occurs for hcp lattices, de Wette[6] has calcu-

lated this number. We have chosen to recalculate it as a check. Terms in the direct lattice sum were included up to $|\sigma_{\lambda j}| = 10$, and the number of terms in the sum were reduced by taking advantage of the threefold symmetry in the hexagonal lattice. The value obtained was $a^3 S^0_{000} = -11.034176$, which is to be compared with de Wette's value[6] of -11.0341754. Similarly, the value obtained for Eq. (A8) was $a^3 S^0_{\frac{1}{3}\frac{1}{3}0} = -23.150541$. The remaining sums, $S^{\lambda_3}_{\frac{1}{3}\frac{1}{3}0}$, $S^{\lambda_3}_{000}$, and $S_{\frac{1}{3}\frac{1}{3}\frac{1}{2}}$ were computed for a range of values in α and inserted in Eqs. (A2a) and (A2b) to yield the curves described in the text. Table III lists some of the results of the calculations. In all cases where possible, comparison of these results with those of Ref. 6 was excellent.

[1] E. N. Kaufmann, second preceding paper, Phys. Rev. B **8**, 1382 (1973).

[2] E. N. Kaufmann, first preceding paper, Phys. Rev. B **8**, 1387 (1973).

[3] J. C. Jamieson, Science **140**, 72 (1963).

[4] S. Andersson, Ark. Kemi **15**, 247 (1960).

[5] R. W. Sommerfeldt, T. W. Cannon, L. W. Coleman, and L. Schecter, Phys. Rev. **138**, B763 (1965); P. H. Stelson and F. K. McGowan, Phys. Rev. **105**, 1346 (1957).

[6] F. W. de Wette, Phys. Rev. **123**, 103 (1961).

[7] F. W. de Wette and G. E. Schacher, Phys. Rev. **137**, A78

(1965); Phys. Rev. **137**, A92 (1965).

[8] R. M. Sternheimer, Phys. Rev. **80**, 102 (1950); Phys. Rev. **84**, 244 (1952); Phys. Rev. **86**, 316 (1954); Phys. Rev. **95**, 736 (1954); Phys. Rev. **105**, 158 (1957); Phys. Rev. **130**, 1423 (1963).

[9] J. E. Doherty and D. F. Gibbons, Acta Metall. **19**, 275 (1971).

[10] L. Pauling, in *Theory of Alloy Phases* (American Society for Metals, Cleveland, 1956).

[11] F. D. Feiock and W. R. Johnson, Phys. Rev. **187**, 39 (1969).

[12] J. Pelzl, Z. Phys. **251**, 13 (1972).

Analysis of the Lattice Specific Heat of Mo:Re Alloy

M. D. Tiwari and Bal K. Agrawal

Department of Physics, University of Allahabad, Allahabad 211002, India

The low-temperature lattice specific heat of a Mo- 5-at.%-Re alloy has been successfully explained on the basis of a Green's-function theory. We take into account the effects due to change in mass at the substitutional impurity site and also the changes in the nearest-neighbor central and noncentral force constants for the impurity–host-crystal interaction. The enhanced specific heat is dominated by force-constant changes and very much sensitive to these changes. It is observed that the contribution of the even parity A_{1g}, E_g, F_{1g}, and F_{2g} modes are very significant and, in fact, dominate over that of F_{1u} symmetry modes in the low-temperature side of the specific-heat curve. However, at higher temperatures more resonance modes appearing in F_{1u} irreducible representation are excited and their contribution dominates over all others. The present values of the defect parameters are found to be quite similar to those obtained earlier by elastic-constant data.

I. INTRODUCTION

The effects of impurities on the vibrational properties of solids has been studied by performing different types of experiments,[1] e.g., measurement of lattice specific heat,[2–4] elastic constants,[5] infrared absorption,[6] inelastic neutron scattering,[7] etc. Usually a localized perturbation model for the defect is assumed to explain these experiments. It is therefore of much interest to determine the defect parameters for a particular host-impurity system which should be able to explain two or more of such experiments. In an earlier work, the elastic constants of Mo:Re alloys measured by Davidson and Brotzen[8] were analyzed by Kesharwani and Agrawal[9] to determine the parameters of a nearest-neighbor-defect model for a rhenium impurity atom in a molybdenum matrix. In the present paper we discuss the lattice-specific-heat measurements made by Morin and Maita[10] on the same system, i.e., Mo:Re (5-at % Re) alloy.

In the specific-heat measurements it is difficult